International Journal of Biological Macromolecules 107 (2018) 212–221

Contents lists available at ScienceDirect

International Journal of Biological Macromolecules

journal homepage: www.elsevier.com/locate/ijbiomac

Research Paper

Chitosan-titanium dioxide-glucantime nanoassemblies effects on promastigote and amastigote of *Leishmania major*

Jaleh Varshosaz[a,*], Bahar Arbabi[a], Nader Pestehchian[b], Sedigheh Saberi[c], Mahdi Delavari[d]

[a] Department of Pharmaceutics, School of Pharmacy and Novel Drug Delivery Systems Research Centre, Isfahan University of Medical Sciences, Isfahan, Iran
[b] Department of Parasitology and Mycology, School of Medicine, Isfahan University of Medical Sciences, Isfahan, Iran
[c] Skin Diseases and Leishmaniasis Research Center, Department of Parasitology and Mycology, School of Medicine, Isfahan University of Medical Sciences, Isfahan, Iran
[d] Department of Parasitology and Mycology, School of Medicine, Kashan University of Medical Sciences, Isfahan, Iran

ARTICLE INFO

Article history:
Received 29 March 2017
Received in revised form 18 July 2017
Accepted 30 August 2017
Available online 1 September 2017

Keywords:
Glucantime
Chitosan
Titanium dioxide nanoparticles
Promastigote
Amastigote
Leishmania major

ABSTRACT

The purpose of the present study was to design nanoassemblies of chitosan-titanium dioxide (TiO_2) nanoparticles (NPs) loaded with glucantime for using their synergistic effects and enhancing the toxic effects of glucantime on *Leishmania* parasites. The nanoassemblies were prepared by electrostatic interactions and optimized by a response surface central composite design. The effects of glucantime, chitosan and TiO_2 NPs amounts were studied on the particle size, zeta potential, loading efficiency, and release efficiency of drug from nanoassemblies. The conjugation of TiO_2/chitosan-glucantime was verified by UV spectroscopy and changes in surface charge of NPs. The anti-promastigots effect of glucantime loaded in TiO_2/chitosan nanoassemblies was studied by tripan blue dye test and their anti-amastigotes effect by counting the average number of parasites per infected J774 macrophages in 100 cells. The optimized formulation obtained by using 12.5 mg glucantime, 25 mg chitosan and 6 mg TiO_2 NPs. Although TiO_2 NPs alone were effective more than negative control in reduction of promastigots and amastigotes but they didn't show significant difference compared with free glucantime ($p > 0.05$). However, at the concentration of 50 μg/mL and after 72 h exposure nanoassemblies decreased the proliferation of *L. major* promastigotes and amastigotes 13 and 4-fold, respectively compared with glucantime alone.

1. Introduction

Metal nanoparticles (NPs) have cytotoxic effects on the different microorganisms due to their small size and their structures that disrupt DNA functions and enzymes and release of ions [1], however, the mechanism of their actions is not well known yet [2]. These NPs act by producing reactive oxygen intermediates that damage cell membrane structures [3].

Titanium dioxide (TiO_2) NPs are used widely in industrial and biological products [4,5]. These NPs are classified as biological harmless and inert materials that are used in many functions. TiO_2 is an FDA approved excipient in drug and food industries and is an ingredient of several oral pharmaceutical dosage forms like tablets or suspensions [6]. TiO_2 NPs have demonstrated widely antibacterial effects due to their activity on oxidative stresses [7]. Producing reactive oxygen species (ROS) by macrophages are taking place in order to destroy virus, fungi and parasites. *Leishmania* parasites survive in macrophages by inhibition of ROS productions via their enzymatic pathway. Metal NPs can overcome this reaction of *Leishmania* parasites and contribute in treatment successes [2]. TiO_2 NPs have strong antibacterial effects against drug resistant bacteria and have cytotoxic effects on *Leishmania* parasites. NPs of Ag/TiO_2 have anti *Leishmanial* effect against *L. tropica* and *L. infantum* [5]. These particles inhibit survival, metabolism and biological activities of *Leishmania* in host cells. Research of Haghi et al. [8] indicated TiO_2 NPs have antibacterial effects on *E. coli*. The investigations of Jebali and Kazemi [2] showed TiO_2 with IR and UV radiation together increase mortality of parasites. However, there is no article that mention the role of TiO_2 nanoassembly with a biological macromolecule like chitosan in drug delivery. TiO_2 has been used in targeted drug delivery of paclitaxel [9] and doxorubicin for enhanc-

* Corresponding author at: Department of Pharmaceutics, Faculty of Pharmacy and Novel Drug Delivery Systems Research Centre, Isfahan University of Medical Sciences, Isfahan, PO Box 81745-359, Iran
E-mail address: varshosaz@pharm.mui.ac.ir (J. Varshosaz).

https://doi.org/10.1016/j.ijbiomac.2017.08.177
0141-8130/

ing the anticancer efficacy and reducing unwanted side effects of these chemotherapeutic drugs [10].

Leishmania is a major global health problem and widespread in 100 countries of the world so that one million new cases are reported each year [11–14]. Pentavalent antimonial (SbV) compounds such as meglumine antimoniate (MA) are still the first line treatment and the choice medicine against *Leishmaniasis*. Glucantime (*N*-methyl glucamine antimoniate) with molecular weight of 365.98 g/mol is a penta valent antimoniate that is highly soluble in water (solubility >300 mg/mL) [15]. In this compound one antimony is associated with *N*-methyl-D-glucosamine molecules and it is thought that acts as a prodrug that is transformed to toxic form of trivalent form (SbIII) in macrophages [16]. For treatment of cutaneous and visceral *Leishmaniasis* 10–20 mg/kg/day of this drug is used for 20–30 days [17,18] in the form of 1500 mg/5 mL injection.

Despite several years of use of these compounds, their mechanism of action, structure, toxicity, pharmacokinetics and ability to damage DNA are still unclear [16,19]. The latest study in this regard was conducted based on radio tracer by neutron irradiation on animals to determine pharmaceutical aspects of these compounds which showed that antimony serum kinetic was bi-exponential, the drug was uptake from liver and eliminated through biliary excretion and kidneys [20].

Antimony compounds have a long duration of treatment course in hospital and have shown clinical resistance especially in HIV patients. They have many side effects including vomiting, arthralgia, and toxic side effects on vital organs such as liver, kidney, heart and pancreas [21]. Due to all these reasons long-term monitoring is required during drug use which makes costs of treatment high. Also drug injection for a prolonged period of 10–20 days leads to poor compliance.

Many studies have been done using nanoparticlulate delivery systems for antileishmania drugs. In a study the effects of pentamidine bound to polymethacrylate was investigated against *Leishmania in vivo* [22,23]. The results showed that 77% of amastigote reduction happened in the treatment group compared with control group. Also several studies have been conducted regarding the effectiveness of Iridium-cyclo-octadiene pentamidine tetraphenyl borate on various species of *Leishmania* [24,25].

Abamor et al. [26] used the combination of TiO_2, Ag Nps and meglumine antimoniate which showed to be much more effective than use of meglumine antimoniate alone at non-toxic concentrations as a new antileishmanial drug to fight against *Leishmaniasis*.

According to available reports on the toxic effects of TiO_2 NPs on *Leishmania* parasites, in the present study it was trying to use a novel macromolecular nanoassembly drug delivery system based on chitosan and without Ag NPs to gain a synergistic effect between TiO_2 and glucantime on promastigote and amastigote forms of *Leishmania major* by using an electrostatic conjugation technique. To our knowledge there is no report on the production of chitosan nanoparticles loaded with glucantime which are electrostatically conjugated to TiO_2 to use of their synergistic effects in suppression of both promastigote and amastigote forms of *Leishmania major* in a sustained release pattern.

2. Material and methods

2.1. Materials

Meglumine antimoniate (Glucantime) was provided from Snofi Aventis (French), low molecular weight chitosan from Sigma Company (US), titanium dioxide nanoparticles from Nanosav Avijeh (Iran), glacial acetic acid and all other reagents were purchased from Merck Chemical Company (Germany). Roswell Park Memorial Institute 1640 medium (RPMI-1640), Novy-MacNeal-Nicolle medium (NNN), fetal bovine serum (FBS), trypsin/EDTA, penicillin/streptomycin were obtained from (Biosera Europe, ZI du Bousquet, France).

2.2. Preparation of nanoassemblies of TiO_2 NPs and glucantime

Nanoassemblies were obtained via an electrostatic conjugation method. Briefly, pure powder of meglumine antimoniate (glucantime) was dissolved in 50 mL of deionized water and added to the solution of chitosan in 0.2% of glacial acetic acid to make a total volume of 100 mL. The mixture was stirred at room temperature for 2 h until completely dissolved. The dispersion of TiO_2 NPs was diluted as a 1% stock solution in 20 mL of deionized water. After that while the solution of drug-chitosan was stirred under ultra-homogenizer (RT10 power IKa® - werke, Germany) at 17,500 rpm, the dispersion of TiO_2 was added drop by drop via a syringe until a yellow transparent dispersion of nanoassemblies was obtained at the end. In order to further reduce the particle size, probe sonication (Bandelin Sonopuls, Germany) was used for 2 min with power of 50%.

Different formulations were designed by Design Expert Software (10.0.4 version, US) using a surface response central composite design with quadratic model, and the optimum formulation was obtained. The amounts of glucantime, chitosan and TiO_2 were changed according to Table 1.

Graphical representation of the prepared nanoassemblies of TiO_2 NPs and glucantime are shown in Fig. 1.

2.3. Characterization of the nanoassemblies of glucantime-chitosan-TiO_2 NPs

2.3.1. Particle size and zeta potential

The particle size, particle size distribution and zeta potential of the prepared nanoparticles were determined by using Zetasizer (Zetasizer-ZEN 3600 Malvern Instrument Ltd., Worcestershire, UK) that works based on dynamic light scattering technique.

2.3.2. Ultra violet analysis of the ingredients

UV spectrum of glucantime, chitosan, glucantime-chitosan, titanium dioxide and prepared nanoassemblies were analyzed in the range of 220–600 nm using a Shimadzue UV-mini1240 spectrophotometer (Japan).

2.3.3. Determination of glucantime content of nanoassemblies

Drug loading efficiency (LE%) was measured by determination of the concentration of free drug in aqueous medium. For this purpose 1 mL of the prepared nanoassemblies was centrifuged at 20,000 rpm for 10 min in micro-centrifuging filter tubes. Amount of antimony was measured by ICP-OES (Inductively Coupled Plasma-Optical Emission Spectrometry) at wavelength of 217.582 nm. The entrapped drug was calculated from the difference between the drug concentration in the filtrated solution (free drug) and the total amount of the applied drug.

$$Loading\ \ efficiency\% \ = \frac{Total\ \ drug - free\ \ drug}{Total\ \ drug} \times 100 \qquad (1)$$

2.3.4. In vitro *release of glucantime from nanoassemblies*

After dialyzing of 2 mL of the nanoassemblies dispersion in dialysis bag with cutoff 12000 Da for an hour against deionized water, the dialysis bag was transferred from water to 20 mL of phosphate buffer solution (PBS) (pH 7.4) and sampling was conducted over 24 h at predetermined intervals. One mL of the medium was taken and the antimony concentration was determined by ICP-OES spectrometry at wavelength of 217.582 nm. The same volume of fresh

Table 1
Formulation of different nanoassemblies of TiO_2 NPs and glucantime.

Formulation code	Glucantime (G) (mg)	Chitosan (C) (mg)	TiO_2 NPs (T) (mg)
$G_{18.75}C_{37.5}T_{4.65}$	18.75	37.5	4.65
$G_{12.5}C_{25}T_{6}$	12.5	25	6
$G_{18.75}C_{19.82}T_{9.25}$	18.75	19.82	9.25
$G_{12.5}C_{50}T_{12.5}$	12.5	50	12.5
$G_{18.75}C_{37.5}T_{9.25}$	18.75	37.5	9.25
$G_{25}C_{50}T_{6}$	25	50	6
$G_{18.75}C_{37.5}T_{13.85}$	18.75	37.5	13.85
$G_{27.59}C_{37.5}T_{9.25}$	27.59	37.5	9.25
$G_{18.75}C_{55.18}T_{9.25}$	18.75	55.18	9.25
$G_{25}C_{25}T_{12.5}$	25	25	12.5
$G_{9.91}C_{37.5}T_{9.25}$	9.91	37.5	9.25

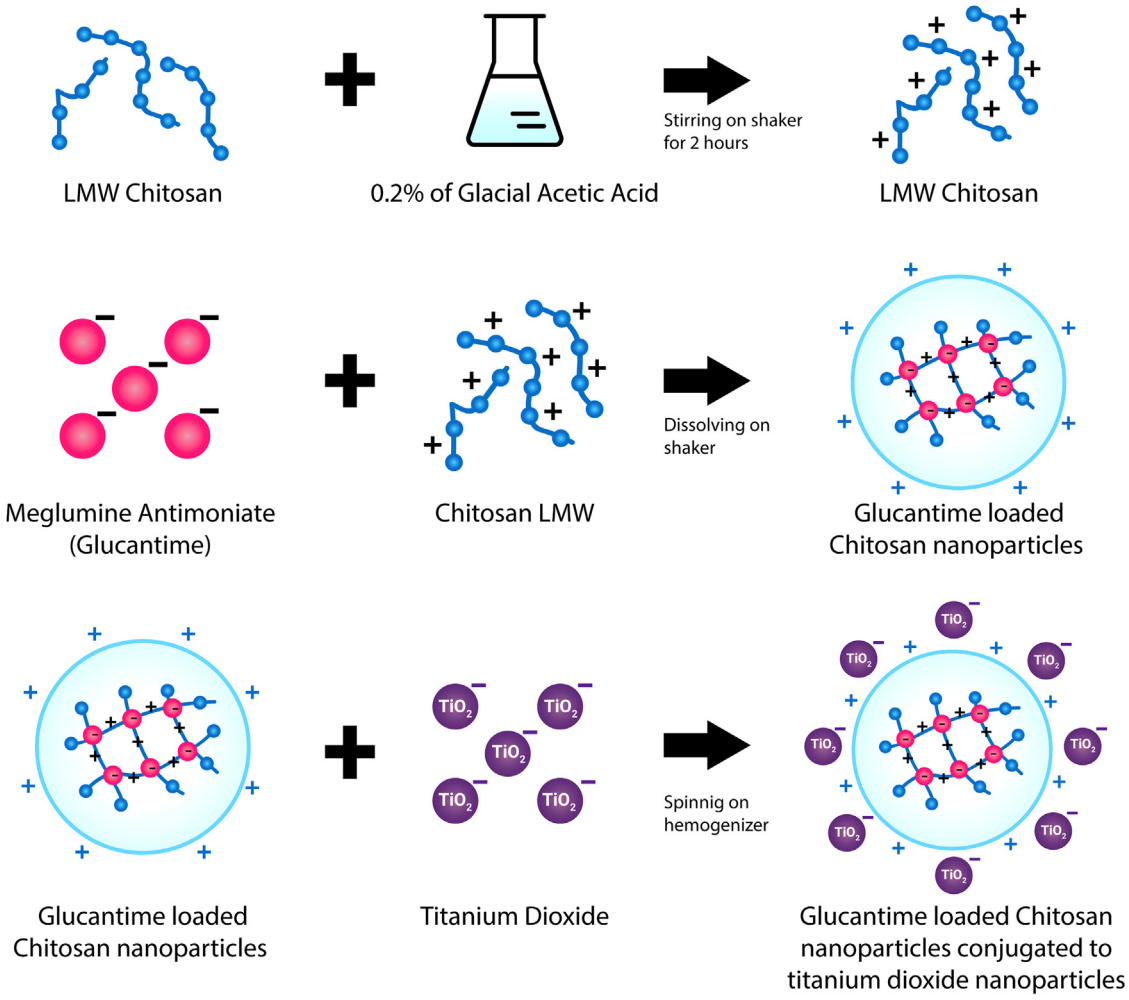

Fig. 1. Graphical representation of the nanoassemblies of glucantime-chitosan-titanium dioxide structure.

buffer was returned to the medium. The antimony release efficiency over 24 h (RE_{24}%) was determined by the following equation:

$$RE_{24}\% \frac{\int_0^t y.dt}{y_{100} \times t} \times 100 \quad (2)$$

2.3.5. Study the particles morphology

The morphology of chitosan-glucantime NPs was studied by Transmission Electron Microscopy (TEM) (Zeiss, EM10C, Germany). To prepare the TEM sample, an appropriate amount of suspension was placed onto a 300 mesh carbon coated copper grid and allowed to dry in air naturally. Finally, micrographs were taken with different levels of magnification with an accelerating voltage of 80 kV.

The morphology of the nanoassemblies of TiO_2 NPs conjugated to chitosan-glucantime were studied by Field Emission Scanning Electron Microscope (FESEM) FESEM (Hitachi, Japan). The samples were prepared by placing a droplet of nanoassemblies dispersion on the microscopy slide and allowing it to dry at room temperature. Before viewing under vacuum conditions, the samples were coated by gold in an argon atmosphere and then tightened on the metal plate with two layers of adhesive tape of copper.

2.4. Leishmania *parasite culture*

L. major (MRHO/IR/75/ER) promastigotes were cultured first in NNN and then RPMI1640 to reach the mass. RPMI-1640 medium

was supplemented with 10% fetal bovine serum (FBS) (Sigma Chemical Co, US), gentamicin (80 μg/mL), penicillin (100 IU/mL) and streptomycin (100 μg/mL) at 25 ± 1° C. The cultures were passaged after 4 days incubation and the growth of promastigotes was monitored daily.

2.5. Anti-promastigote assay

In order to assess inhibitory concentration of nanoassemblies on *L. major*, 96 well plates were used. Each well contained 100 μL of the medium, antibiotics and 1×10^6 parasites in stationary phase. Then parasites were treated in different groups: 1) nanoassemblies (166.50, 83.25, 41.62 μg/mL) containing the same concentrations of pure glucantime used in the third group, 2) only TiO_2 NPs (33.72, 16.86, 8.43 μg/mL), 3) only glucantime (50, 25, 12.5 μg/mL) as positive control and 4) no treatment as the negative control. The concentrations of TiO_2 NPs were selected according to the amounts of this substance present in different concentrations of nanoassemblies. Each test was repeated in triplicate and the wells were incubated at 24 °C and were evaluated after 24, 48 and 72 h. Then the promastigotes were counted using 0.4% tripan blue dye on a Neubauer haemocytometer counting chamber.

2.6. J774 macrophage cell culture

J774 mouse macrophage cell-line was grown in a 37 °C culture flasks with RPMI-1640 supplemented with 10% fetal bovine serum (FBS), penicillin (100IU/mL) and streptomycin (100 μg/mL). Cells were passaged when they reached 70% confluence.

2.7. Anti-amastigotes assay

J774 macrophage cells (2×10^6 cells/mL) were seeded in 6 well plates. At the bottom of every well a sterile coverslip was located. The plates were incubated at 37 °C for 24 h. Macrophage cells were then infected with *L. major* promastigotes at a parasite/macrophage ratio of 7:1 and incubated at 37 °C in 5% CO_2 for 24 h. Free promastigotes were washed out of wells with PBS and different concentrations of 1) nanoassemblies (166.50, 83.25, 41.62 μg/mL) which contained the same concentrations similar to free glucantime concentrations, 2) only TiO_2 (33.72, 16.86, 8.43 μg/mL) and 3) only free glucantime (50, 25, 12.5 μg/mL) based on the Ed_{50} obtained in preliminary studies, were added to the containers. The fourth group received no treatment as the negative control. At three different time intervals (24, 48 and 72 h) the results were viewed and the coverslips were fixed with methanol, stained with 10% Giemsa and added oil-immersion light microscopy for examining. The number of infected macrophages and the average number of parasites per macrophage were counted in 100 cells.

2.8. Statistical analysis

Values were processed by Microsoft Excel 2017 and IBM SPSS Statistics (Ver. 18, US) for determination of significant difference between variables. Analysis of variance test (ANOVA) followed by the post hoc test of LSD was done and the level of significance was set at P values < 0.05.

3. Results

3.1. Particle size and zeta potential

The particle size distribution of nanoassemblies of TiO_2 NPs and chitosan-glucantime were determined by a dynamic light scattering (DLS) instrument. The results showed the mean particle size of 170 nm with a polydispersity index (PDI) of 0.4 in optimum formulation ($G_{12.5}C_{25}T_6$) which shows low diversity of particle size. The surface charge is an important physicochemical feature of NPs that is determined by changing zeta potential. The zeta potential of chitosan was +70 mV and when glucantime was added to it, it changed to +61 mV that shows glucantime with negative charge was conveniently cross-linked the chitosan with opposite charge. Finally when TiO_2 NP_s were added to chitosan-glucantime NPs, the zeta potential changed to +48 mV. Zeta potential of TiO_2 NPs alone was −59.4 mV which indicates that they can be assembled and make complex with positive charge of chitosan-glucantime NPs. The results of changing the zeta potential clearly show the production of nanoassemblies by electrostatic forces. Besides the UV spectrum of nanoassembelies was studied to confirm the electrostatic conjugation of chitosan-glucantime with TiO_2 NPs. UV–vis spectra of glucantime, chitosan, glucantime-chitosan, titanium dioxide and the nanoassemblies are shown in Fig. 2. This figure shows a single broad UV absorption peak at 259 nm for TiO_2, while no absorption peak for glucantime, chitosan and glucantime-chitosan NPs. Similar to TiO_2, glucantime-chitosan-TiO_2 nanoassemblies displayed a relatively high UV−vis absorbance in the same wavelength, and the shift of the characteristic peak from 252 nm in TiO_2 to 259 nm in nanoassemblies suggests conjugation of TiO_2 to glucantime-chitosan NPs.

The results of physicochemical properties of different formulations of nanoassemblies are shown in Table 2. The particle size and the PDI of different formulations was between 170.56–853.43 nm and 0.19–0.55, respectively.

Analysis of the results of Table 2 by Deign Expert Software showed a linear model was best fitted to the results of particle size and a quadratic model to zeta potential of nanoassemblies ($P < 0.05$). The concentrations of chitosan and TiO_2 had significant effect on particle size ($P < 0.0001$) so that, by increasing the amount of both these variables the particle size of nanoassemblies increased (Table 2). All the studied variables had also significant effects on the zeta potential of nanoassemblies ($P < 0.05$).

3.2. Determination of antimony loaded in nanoassemblies of TiO_2 NPs and chitosan-glucantime

ICP-OES analysis at wavelength of 217.582 nm was used for determining of antimony in the prepared nanoassemblies. The concentration of antimony in the optimum formulation of nanoassemblies ($G_{12.5}C_{25}T_6$) was 68.22%. The results of Table 2 showed the loading efficiency of formulations were between 67 and 78%. The best model fitted to the results of the loading efficiency was a quadratic model ($P < 0.05$). The concentration of glucantime had a significant increasing effect on the loading efficacy ($P < 0.05$). However, the effects of chitosan and TiO_2 concentrations was not significant on the loading efficacy ($P > 0.05$) (Table 2).

3.3. In vitro release of glucantime from nanoa ssemblies of TiO_2 NPs and chitosan-glucantime

The release profile of antimony versus time was measured by ICP-OES analysis in the wavelength of 217.582 nm for the prepared nanoassemblies in 11 formulations (Fig. 3). In the optimum formulation ($G_{12.5}C_{25}T_6$) 82.73% of the loaded antimony was released within 24 h. The results of Table 2 show the release efficiency of the drug over 24 h for different formulations. Analysis of data showed that the concentration of components of nanoassenblies did not have significant effect on the release efficiency of glucantime ($P > 0.05$).

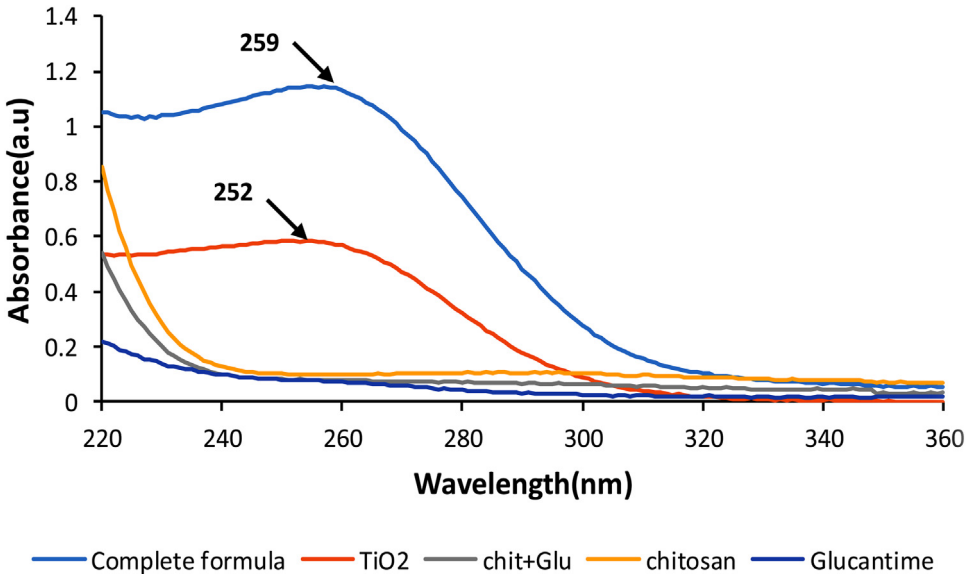

Fig. 2. UV–vis spectrum of glucantime, chitosan, glucantime-chitosan, titanium dioxide and the nanoassemblies.

Table 2
Particle size, zeta potential, loading efficiency and release efficiency of glucantime over 24 h (RE_{24}%) from nanoassemblies of TiO_2 NPs and glucantime.

PdI ± SD	RE_{24}% ± SD	Drug release% over 24 h	Loading efficiency% ± SD	Zeta potential (mV) ± SD	Mean particle size (nm) ± SD	Formulation code
0.41 ± 0.02	44.8 ± 9.8	45.6	70.4 ± 1.5	+71.4 ± 5.3	400.8 ± 43.3	$G_{18.75}C_{37.5}T_{4.65}$
0.38 ± 0.05	63.0 ± 10.0	82.7	68.2 ± 1.6	+42.8 ± 8.7	170.6 ± 22.7	$G_{12.5}C_{25}T_{6}$
0.34 ± 0.03	37.4 ± 3.4	31.2	76.3 ± 0.8	+64.2 ± 7.44	365.8 ± 53.0	$G_{18.75}C_{19.82}T_{9.25}$
0.42 ± 0.07	33.5 ± 10.0	41.3	73.3 ± 1.1	+78.1 ± 2.27	649.6 ± 15.1	$G_{12.5}C_{50}T_{12.5}$
0.38 ± 0.00	49.5 ± 3.7	65.1	76.2 ± 1.8	+72.6 ± 2.30	522.4 ± 6.2	$G_{18.75}C_{37.5}T_{9.25}$
0.37 ± 0.04	47.3 ± 13.0	42.3	73.2 ± 0.7	+70.8 ± 3.0	365.0 ± 10.9	$G_{25}C_{50}T_{6}$
0.44 ± 0.06	55.2 ± 10.0	53.6	73.5 ± 0.8	+77.9 ± 2.1	853.4 ± 64.5	$G_{18.75}C_{37.5}T_{13.85}$
0.24 ± 0.17	69.9 ± 10.0	74.6	77.1 ± 2.0	+70.3 ± 1.5	578.6 ± 51.9	$G_{27.59}C_{37.5}T_{9.25}$
0.37 ± 0.06	41.3 ± 20.0	40.0	73.5 ± 1.0	+71.2 ± 0.4	753.0 ± 28.6	$G_{18.75}C_{55.18}T_{9.25}$
0.55 ± 0.16	94.0 ± 8.0	100.0	77.7 ± 0.9	+74.5 ± 0.6	662.1 ± 51.1	$G_{25}C_{25}T_{12.5}$
0.19 ± 0.08	75.2 ± 1.1	75. 9	67.2 ± 2.0	+57.3 ± 1.6	509.3 ± 21.4	$G_{9.91}C_{37.5}T_{9.25}$

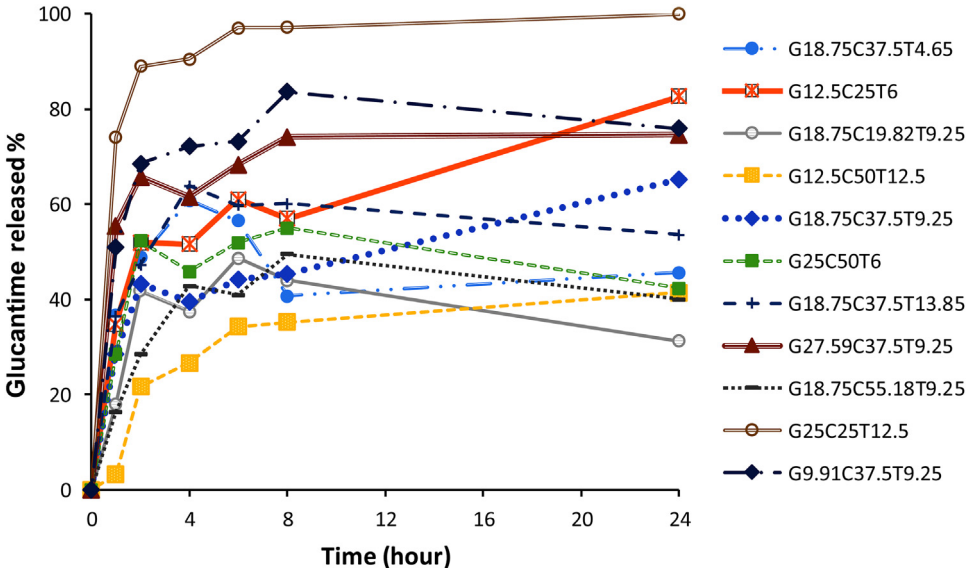

Fig. 3. Release profiles of different formulations of the nanoassemblies.

3.4. Optimization of the formulation of nanoassemblies

Computer optimization process was performed using Design Expert software and a desirability function determined the effect of the levels of independent parameters on the responses. Table 2 displays that the constraint of particle size was 170.6 ± 22.7 nm ≤ Y1 ≤ 853.4 ± 64.5 nm with the goal set on minimum. For zeta potential it was 42.8 ± 8.7 mV ≤ Y2 ≤ 78.1 ± 2.27 mV and it was set at the range of the data, for drug loading efficiency the constraint was 68.2 ± 1.6% ≤ Y3 ≤ 77.7 ± 0.9% with targeting this

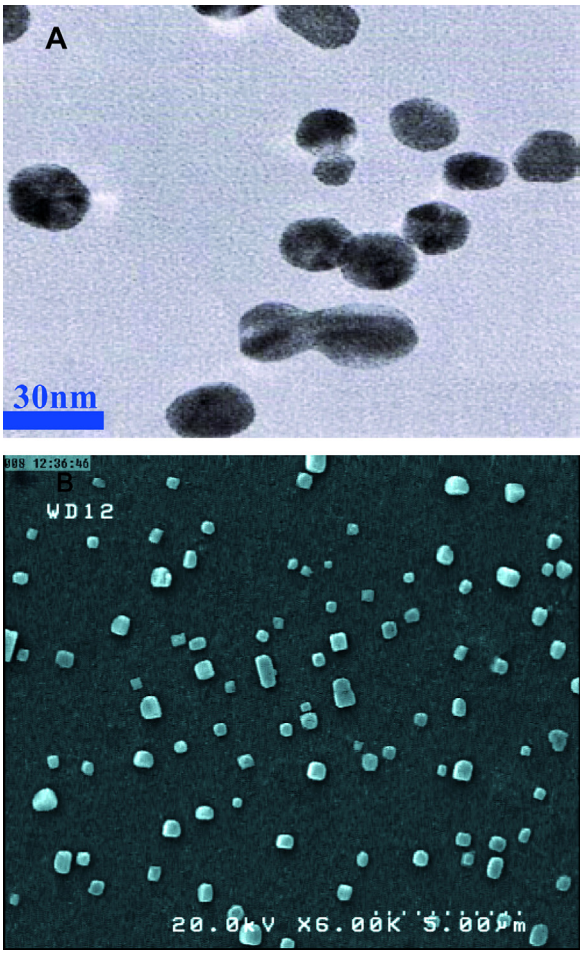

Fig. 4. A) TEM image of chitosan loaded NPs and B) the FE-SEM micrograph of nanoassemblies of chitosan-glucantime-TiO_2.

variable in the range of the data and the RE_{24}% constraint was $33.5 \pm 10.0\% \leq Y4 \leq 94.0 \pm 8.0\%$ with the target set on maximum. Optimization was performed and the optimized formulation was suggested by desirability of 95%. The suggested formulation was $G_{12.5}C_{25}T_6$, which was prepared with 12.5 mg of glucantim, 25 mg of chitosan and 6 mg of TiO_2 NPs.

3.5. Morphology of chitosan-glucanthime NPs and nanoassemblies of chitosan-glucantime-TiO_2 NPs

Fig. 4 shows the TEM image of chitosan-glucantime NPs and the FE-SEM micrograph of nanoassemblies of chitosan-glucantime-TiO_2. This figure indicates the chitosan nanoparticles loaded with glucantime have spherical shapes with particle sizes less than 30 nm and when they are electrostatically conjugated to TiO_2 NPs the morphology changed to square, angled form.

3.6. Cytotoxic effect of free glucantime, TiO_2 NPs and nanoassemblies on L. major promastigotes

Analysis of the results of the growth of promastigotes in three time intervals and in the presence of different concentrations of free glucantime, TiO_2 NPs and nanoassemblies showed that the time of exposure and also the concentration of different studied groups had significant effect on the proliferation of promastigotes (Fig. 5). All concentrations of the studied groups showed significant difference with negative control group ($P < 0.05$). It was obvious that all different concentrations of nanoassemblies showed significantly more anti-proliferative effect in comparison with free glucantime ($p < 0.05$). Their highest suppressive effect was seen at the concentration of 50 μg/mL according to the pure content of glucantime after 24 h which was 358,000 for free glucantime and 10,000 for nanoassemblies compared with 1,100,000 in negative control group. However, none of the concentrations of TiO_2 NPs had considerable impact on promastigotes proliferation in comparison with free glucantime ($P < 0.05$). Compared to the negative control group TiO_2 NPs were significantly more effective in reduction of the number of promastigots at all times of exposure and all studied concentrations ($p < 0.05$) (Fig. 5).

3.7. Cytotoxic effect of free glucantime, TiO_2 NPs and nanoassemblies on L. major amastigotes

Results of Fig. 6 indicate that different studied time intervals of exposure and different concentrations of each group had significant effects on the amastigotes proliferation ($p < 0.05$). All the studied groups, including nanoassemblies, TiO_2 NPs and free glucantime had significant difference with negative control group ($p < 0.05$). The best suppressive effect of nanoassemblies on parasites was at the concentration of 166.5 μg/mL (containing 50 μg/mL of free glucantime) after 72 h which was significantly better than the same concentration of free glucantime ($p < 0.05$). Also the concentration of 83.25 μg/mL of nanoassemblies (containing 25 μg/mL of free glucantime) had a better anti-proliferative effect in comparison with the same concentration of the free drug ($p < 0.05$). Although the different concentrations of TiO_2 NPs reduced the number of amastigotes counting compared with negative control group significantly ($p < 0.05$), but a significant decrease in the number of amastigotes counting was not seen in comparison with free glucantime as the positive control group ($p > 0.05$) (Fig. 6).

Fig. 7 represents visible light microscopy images of infected macrophage cells with amastigotes after incubation with nanoassemblies, TiO_2 NPs and glucantime in the concentration of 50 μg/mL in three different times exposure of 24, 48 and 72 h. As this figure indicates at 72 h although in the groups of free glucantime and TiO_2 NPs the number of amastigotes has reduced compared to the negative control group, but the nanoassemblies have destroyed the infected macrophages completely so that their elongated shape and their false feet has diminished completely.

4. Discussion

Metal nanoparticle ions have cytotoxic effects as the Leishmanicidal agents due to their activities on oxidative stress which destroys parasites [7]. Also meglumine antimoniate (glucantime) despite of all its problems and side effects is still the first and gold standard of treatment of *Leishmaniasis* [27]. Therefore, many researches have been done to improve its efficacy and decrease its side effects and drug resistance. In the current study nanoassemblies of glucantime-chitosan and TiO_2 NPs were prepared by electrostatic interactions with loading efficiency of about 70% and drug release of 83% over a 24 h period. To confirm the electrostatic interaction between the TiO_2 NPs and chitosan, the UV spectrum of different ingredients of the nanoassemblies were compared with the conjugate (Fig. 2). TiO_2 is widely used in sunscreen products and often in combination with chemical UV-filters. Two crystalline forms, anatase and rutile, are available in different particle sizes, with particles under 100 nm classified as nanoparticles, and the larger particles as microparticles. Each particle size has a different wavelength in UV range. Therefore, we used the same properties of TiO_2 NPs to prove their binding to chitosan. The change in the UV absorption peak of TiO_2 NPs from 252 nm to 259 nm in the nanoassemblies of chitosan-glucantime-TiO_2 NPs confirms

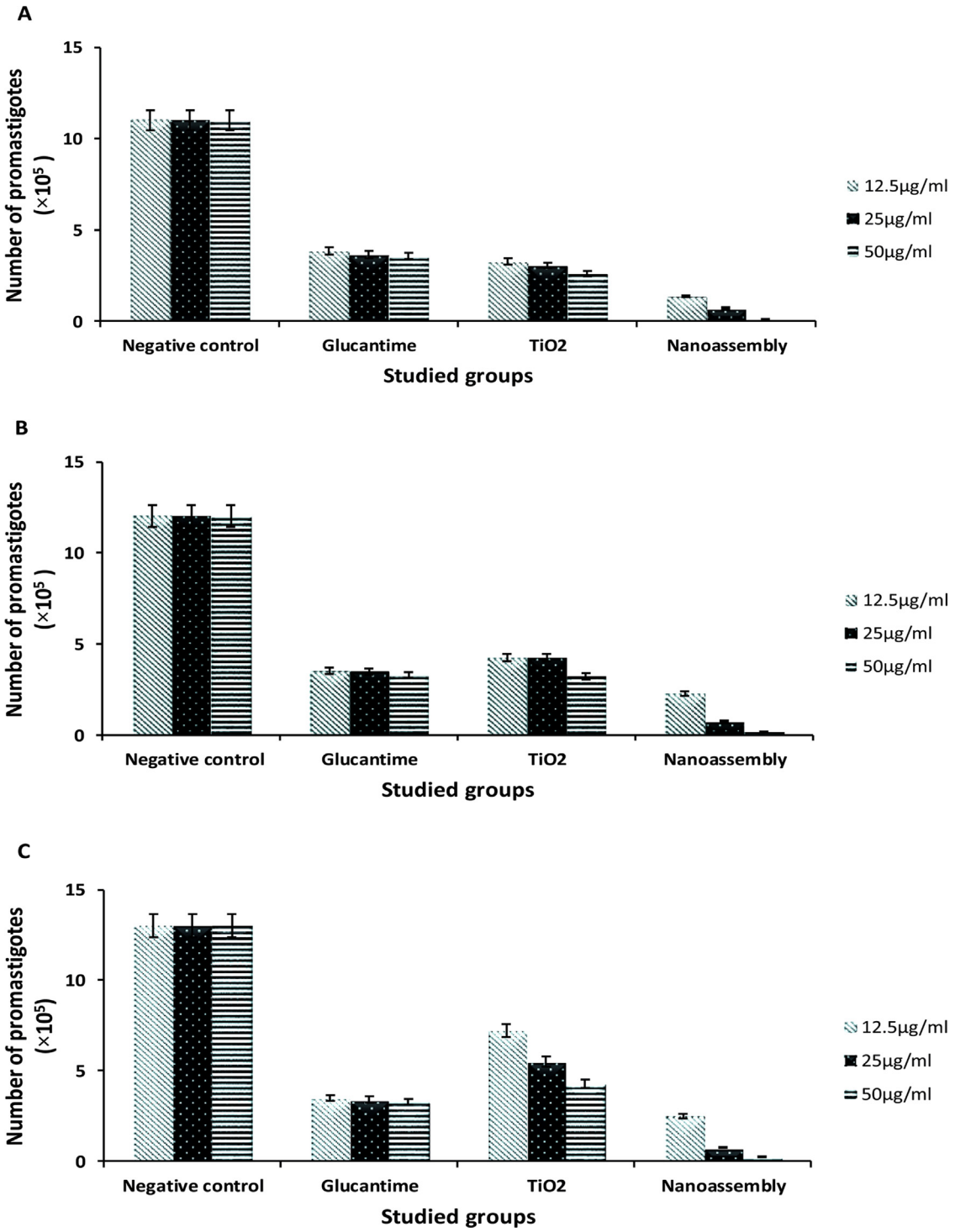

Fig. 5. Mean number ($\times 10^5$) of promastigotes in different concentrations of nanoassemblies, TiO_2 NPs and glucantime in the three different times exposure of A) 24 h, B) 48 h and C) 72 h.

the electrostatic conjugation of these NPs (Fig. 2). In a study conducted by Venkatasubbu et al. [28] paclitaxel, an anticancer drug, was attached to functionalized hydroxyapatite and titanium dioxide nanoparticles and then the conjugates were characterized with their UV spectroscopy to confirm the successful attachment of the drug to NPs.

Low molecular weight chitosan that is a water-soluble cationic polymer was used as a biological macromolecule intermediate. This polymer has been studied widely and has been considered biocompatible and biodegradable with a good stability [29]. The presence of multiple amino functional groups in the backbone of this polymer enhances the electrostatic entrapment of glucantime in chitosan NPs through the interaction of the positive zeta potential of chitosan with the negative charge of the glucantime. The results showed that the zeta potential of chitosan changed from +70 mV to +61 mV when conjugated to the glucantime which shows neutralization of some parts of the positive charge of chitosan with negative glucantime. At last attachment of TiO_2 NPs with

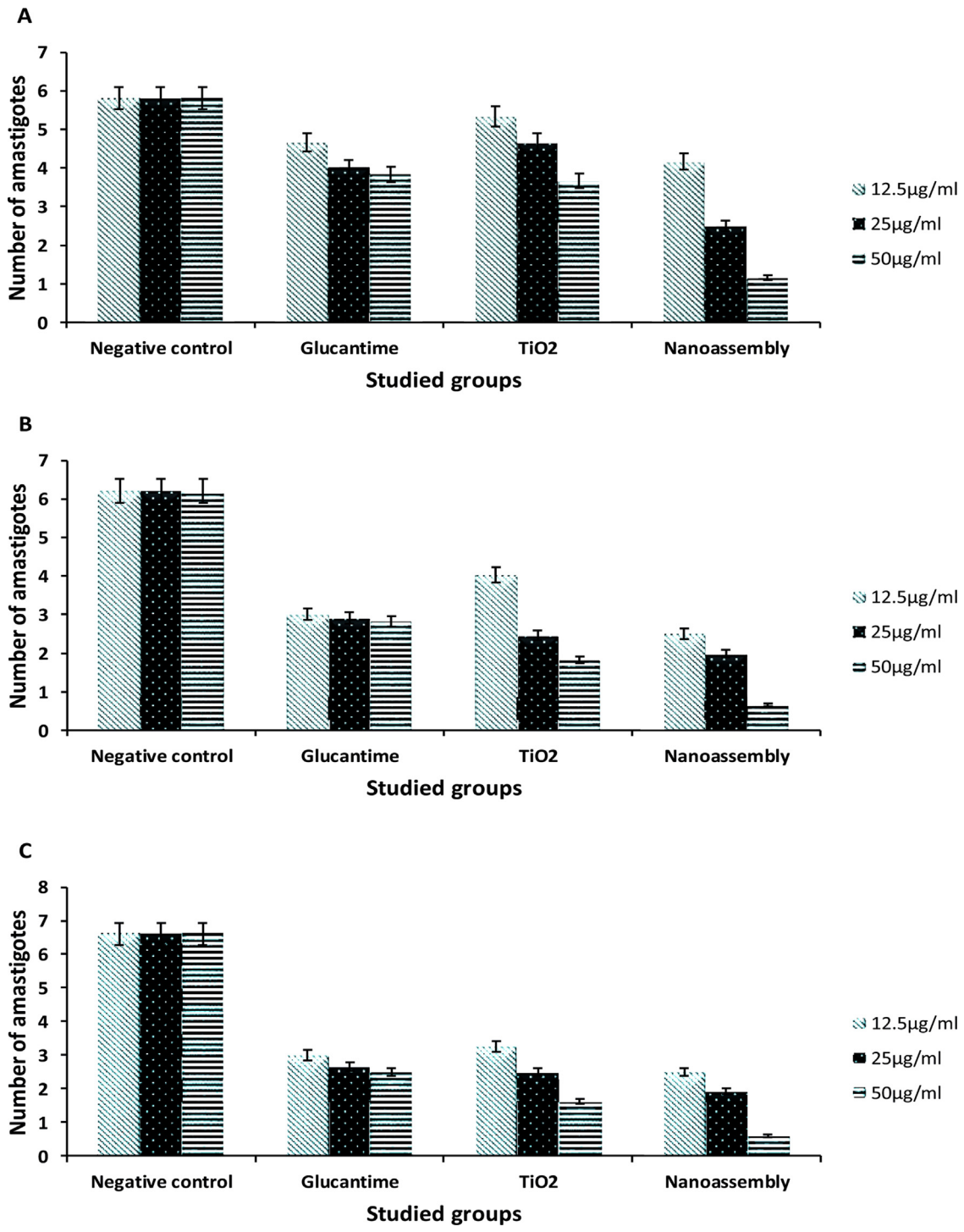

Fig. 6. Mean number of amastigotes per macrophage in different concentrations of nanoassemblies, TiO_2 NPs and glucantime in the three different times exposure of A) 24 h, B) 48 h and C) 72 h.

zeta potential of −59.4 mV changed this positive surface charge from +61 mV to +48 mV which confirmed the production of self-assemblies via electrostatic forces. In a similar study in which the anti-tumor drug of doxorubicin was electrostatically conjugated to TiO_2 NPs to use their synergistic anticancer effects, the surface charge of TiO_2 NPs changed from −26 mV to −5 mV due to the positive NH_2 functional group of doxorubicin [1,10].

TiO_2 NPs were used to produce a synergistic effect with glucantime by producing reactive oxygen species that improves the activity of macrophages and facilitates the efficacy of glucantime effects on parasites. Beheshti et al. [30] studied the efficacy of selenium NPs against *Leishmania major*. Their results showed significant reduction in the number of promastigotes in present of selenium NPs. Also the cytotoxic studies on the infected macrophages showed a dose-dependent response and highlighted IC_{50} for the selenium NPs at the concentration of 10.5 ± 0.6 µg/mL. Allahverdiy et al. [31] studied the effect of silver (Ag) NPs under ultraviolet (UV) light on the *Leishmania tropica*. The metabolic activity of parasite decreased with the increase of concentration of Ag NPs [31]. A similar study was conducted with these NPs combined

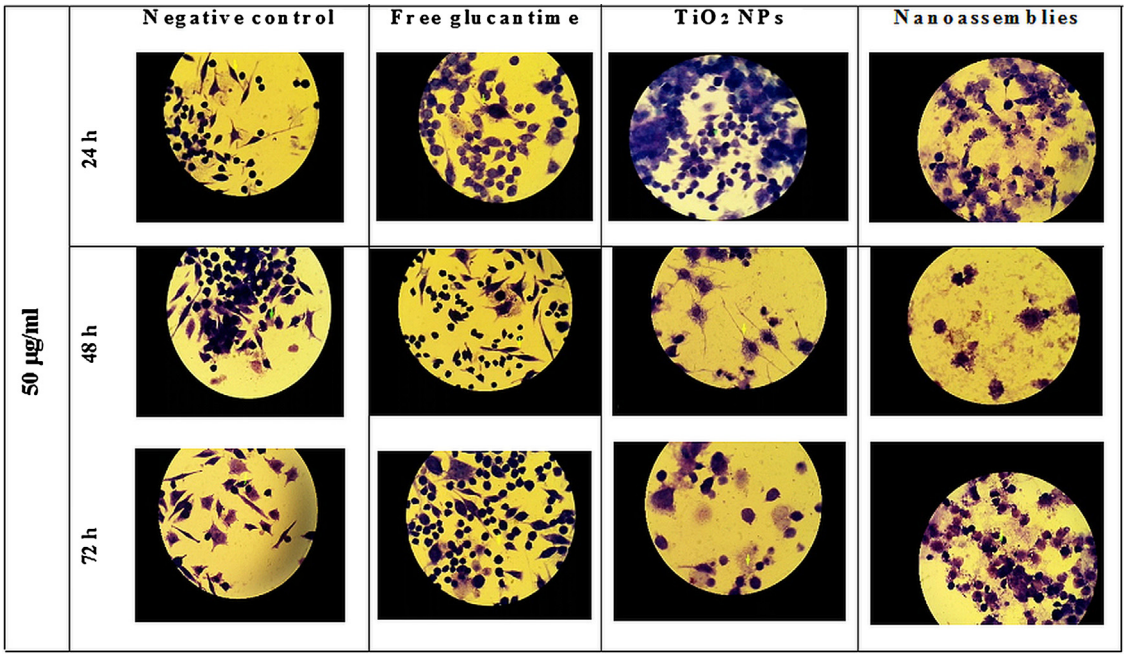

Fig. 7. Visible light microscopy images of infected macrophage cells with amastigotes after incubation with nanoassemblies, TiO_2 NPs and glucantime in the concentration of 50 μg/mL in the three different times exposure of 24, 48 and 72 h.

with the effect of UV radiation on animal models [32]. The antileishmaniasis effect of ZnO NPs on the amastigote and promastigotes of *Leishmania major* has been also shown [33]. Torabi et al. [34] have studied on gold NPs and showed these NPs possessed antileishmania activity on *Leishmania major*.

When the infected female Sandfly bites the human body, the life cycle of the leishmania parasite begins. Promastigots which are extracellular flagellated and animated spiny figure bodies with length of 20–25 μm and width of 3–2 μm are swallowed within a few minutes by phagocytes, ie, macrophages and neutrophils. Due to the short life span of neutrophils, macrophages are the main host of the leishmania parasite, where they multiply. After promastigotes are swallowed by macrophages, they enter the phagolysosomes, where they begin to differentiate and become immobilized small amastigotes with length of 2–4 μm and without flagellum. Amastigotes rapidly proliferate and cause macrophage tearing and contamination of macrophages around them. Although Leishmania parasites in the infected host interact with a variety of cell types, it could be said that macrophages and dendritic cells are the most important cells that control the infection outcome [35].

The designed nanoassemblies of glucantime-chitosan-TiO_2 in the current study were exposed to the J774 cell line that acts like human macrophages in a condition most similar to the human body and their antileishmanial effects on amastigotes of *Leishmania major* was shown (Figs. 6 and 7). The increased drug penetration into the macrophage cells was confirmed by enhanced anti-proliferative effects on amastigotes compared with the free glucantime (Fig. 6). Although the number of promastigotes in negative control group increased over times of the study but this process was slowed done in the group exposed to the nanoassemblies.

All studied groups including the designed nanoassemblies, TiO_2 NPs and free glucantime significantly inhibited the growth of amastigotes and promastigotes in comparison with negative control group ($p < 0.05$) (Figs. 5 and 6). The equal concentration of nanoassemblies of drug compared with the free glucantime (50 μg/mL) showed obviously more effectiveness of nanoassemblies on reduction of the amastigotes count ($p < 0.05$) (Figs. 6 and 7). Although titanium dioxide was more effective than negative control in reduction of amastigotes but it didn't show significant difference compared with free glucantime ($p > 0.05$) (Fig. 6). This shows that nanoassemblies of drug have more effectiveness than each free glucantime or TiO_2 NPs alone.

Abamor et al. study [26] who used the combinations of meglumine antımoniate-TiO_2@Ag nanoparticles demonstrated that combination applications decreased the proliferation of *L. topica* promastigotes 2- to 5-fold in contrast to use of meglumine antımoniate alone. The results of Figs. 5 C and 6 C shows by incorporating of glucantime and TiO_2 in a biomacromolecule like chitosan at the concentration of 50 μg/mL and after 72 h exposure the proliferation of *L. major* promastigotes and amastigotes decreased 13 and 4-fold, respectively compared with glucantime alone.

5. Conclusions

The optimized nanoassemblies of glucantime-chitosan-titanium dioxide prepared by electrostatic surface charge interactions showed particle size of 170.6 ± 22.7 nm, polydispersity index of 0.38 ± 0.05 and zeta potential of $+42.8 \pm 8.7$ mV. These nanoassemblies with $68.2 \pm 1.6\%$ drug loading efficiency released 82.7% of the loaded drug over 24 h. The *in vitro* antileishmanial effect of these nanoassembleis indicated that they were much more effective than free glucantime and/or titanium dioxide alone in reduction of promastigots and amastigots.

Acknowledgment

The authors appreciate financial support of Isfahan University of Medical Sciences.

References

[1] Y. Chen, Y. Wan, Y. Wang, H. Zhang, Z. Jiao, Anticancer efficacy enhancement and attenuation of side effects of doxorubicin with titanium dioxide nanoparticles, Int. J. Nanomed. 6 (2011) 2321–2326.
[2] A. Jebali, B. Kazemi, Nano-based antileishmanial agents: a toxicological study on nanoparticles for future treatment of cutaneous leishmaniasis, Toxicol. In Vitro 27 (6) (2013) 1896–1904.

[3] M. Heinlaan, A. Ivask, I. Blinova, H.C. Dubourguier, A. Kahru, Toxicity of nanosized and bulk ZnO, CuO and TiO_2 to bacteria Vibrio fischeri and crustaceans Daphnia magna and Thamnocephalusplatyurus, Chemosphere 71 (7) (2008) 1308–1316.
[4] A. Kahru, H.C. Dubourguier, I. Blinova, A. Ivask, K. Kasemets, Biotests and biosensors for ecotoxicology of metal oxide nanoparticles: a mini review, Sensors 8 (8) (2008) 5153–5170.
[5] A.M. Allahverdiyev, E.S. Abamor, M. Bagirova, S.Y. Baydar, S.C. Ates, F. Kaya, C. Kaya, M. Rafailovich, Investigation of antileishmanial activities of Tio2@Ag nanoparticles on biological properties of *L. tropica* and *L. infantum* parasites, *in vitro*, Exp. Parasitol. 135 (2013) 55–63.
[6] M. Skocaj, M. Filipic, J. Petkovic, S. Novak, Titanium dioxide in our everyday life; is it safe? Radiol. Oncol. 45 (4) (2011) 227–247.
[7] A.M. Allahverdiyev, E.S. Abamor, M. Bagirova, M. Rafailovich, Antimicrobial effects of TiO_2 and Ag_2O nanoparticles against drug-resistant bacteria and leishmania parasites, Future Microbiol. 6 (8) (2011) 933–940.
[8] M. Haghi, M. Hekmatafshar, M.B. Janipour, S.S. Gholizadeh, M.K. Faraz, F. Sayyadifar, M. Ghaedi, Antibacterial effect of TiO_2 nanoparticles on pathogenic strain of *E. coli*, Int. J. Adv. Biotechnol. Res. 3 (3) (2012) 621–624.
[9] G.D. Venkatasubbu, S. Ramasamy, V. Ramakrishnan, J. Kumar, Folate targeted PEGylated titanium dioxide nanoparticles as a nanocarrier for targeted paclitaxel drug delivery, Adv. Powder Technol. 24 (6) (2013) 947–954.
[10] Y. Chen, Y. Wan, Y. Wang, H. Zhang, Z. Jiao, Anticancer efficacy enhancement and attenuation of side effects of doxorubicin with titanium dioxide nanoparticles, Int. J. Nanomed. 6 (2011) 2321–2326.
[11] B.M. Valencia, D. Miller, R.S. Witzig, A.K. Boggild, A. Llanos-Cuentas, Novel low-cost thermotherapy for cutaneous leishmaniasis in Peru, PLoS Negl. Trop. Dis. 7 (2013) 1–9.
[12] J.A. Makwali, F.M.E. Wanjala, J.C. Kaburi, J. Ingonga, W.W. Byrum, C.O. Anjili, Combination and monotherapy of Leishmania major infection in BALB/c mice using plant extracts and herbicides, J. Vector Borne Dis. 49 (2012) 123–130.
[13] T. Garnier, S.L. Croft, Topical treatment for cutaneous leishmaniasis, Curr. Opin. Investig. Drugs 3 (4) (2002) 538–544.
[14] S.L. Croft, K. Seifert, V. Yardley, Current scenario of drug development for leishmaniasis, Indian J. Med. Res. 123 (2006) 399–410.
[15] P.S. Martins, R. Ochoa, A.M. Pimenta, L.A. Ferreira, A.L. Melo, J.B. da Silva, R.D. Sinisterra, C. Demicheli, F. Frézard, Mode of action of beta-cyclodextrin as an absorption enhancer of the water-soluble drug meglumine antimoniate, Int. J. Pharm. 325 (1–2) (2006) 39–47.
[16] M.I. Lima, V.O. Arruda, E.V. Alves, A.P. de Azevedo, S.G. Monteiro, S.R. Pereira, Genotoxic effects of the antileishmanial drug glucantime, Arch. Toxicol. 84 (3) (2010) 227–232.
[17] R. Firdous, M. Yasinzai, K. Ranja, Efficacy of glucantime in the treatment of Old World cutaneous leishmaniasis, Int. J. Dermatol. 48 (7) (2009) 758–762.
[18] P.J. Guerin, P. Olliaro, S. Sundar, M. Boelaert, S.L. Croft, P. Desjeux, M.K. Wasunna, A.D. Bryceson, Visceral leishmaniasis: current status of control diagnosis, and treatment, and a proposed research and development agenda, Lancet Infect. Dis. 2 (8) (2002) 494–501.
[19] F. Frézard, C. Demicheli, New delivery strategies for the old pentavalent antimonial drugs, Expert Opin. Drug Deliv. 7 (2010) 1343–1358.
[20] S.E.T. Borborema, J.A.O. Junior, H.F.D. Andrade, N.D. Nascimento, Biodistribution of meglumine antimoniate in healthy and *Leishmania* (*Leishmania*) *infantum chagasi*-infected BALB/c mice, Mem. Inst. Oswaldo Cruz 108 (5) (2013) 623–630.
[21] E.O. Freitas, D. Nico, M.V. Alves-Silva, A. Morrot, K. Clinch, G.B. Evans, P.C. Tyler, V.L. Schramm, C.B. Palatnik-de-Sousa, Immucillins ImmA and ImmH are effective and non-toxic in the treatment of experimental visceral Leishmaniasis, PLoS Negl. Trop. Dis. 9 (12) (2015) e0004297.
[22] T. Fusai, M. Deniau, R. Durand, C. Bories, M. Paul, D. Rivollet, A. Astier, R. Houin, Action of pentamidine-bound nanoparticles against Leishmania on an *in vivo* model, Parasite 1 (4) (1994) 319–324.
[23] R. Durand, M. Paul, D. Rivollet, R. Houin, A. Astier, M. Deniau, Activity of pentamidine-loaded methacrylate nanoparticles against Leishmania *infantum* in a mouse model, Int. J. Parasitol. 27 (11) (1997) 1361–1367.
[24] P.M. Loiseau, G. Dreyfuss, S. Daulouède, G. Lachâtre, P. Vincendeau, D.G. Craciunescu, Trypanocidal effect of Ir-(COD)-pentamidine tetraphenylborate on Trypanosoma brucei and T. b gambiense rodent models and serum kinetics in sheep, Trop. Med. Int. Health 2 (1) (1997) 19–27.
[25] P.M. Loiseau, N. Mbongo, C. Bories, Y. Boulard, D.G. Craciunescu, In vivo antileishmanial action of Ir-(COD)-pentamidine tetraphenylborate on Leishmania donovani and Leishmania major mouse models, Parasite 7 (2) (2000) 103–108.
[26] E.S. Abamor, A.M. Allahverdiyev, M. Bagirova, M. Rafailovich, Meglumine antımoniate-TiO2@Ag nanoparticle combinations reduce toxicity of the drug while enhancing its antileishmanial effect, Acta Trop. 169 (2017) 30–42.
[27] R. Hadighi, M. Mohebali, P. Boucher, H. Hajjaran, A. Khamesipour, M. Ouellette, Unresponsiveness to glucantime treatment in Iranian cutaneous leishmaniasis due to drug-resistant *Leishmani tropica* parasites, PLoS Med. 3 (5) (2006) e162.
[28] G.D. Venkatasubbu, S. Ramasamy, G.P. Reddy, J. Kumar, *In vitro* and *In vivo* anticancer activity of surface modified paclitaxel attached hydroxyapatite and titanium dioxide nanoparticles, Biomed. Microdevice 15 (4) (2013) 711–726 https://link.springer.com/journal/10544/15/4/page/1.
[29] L. Liu, X. Dong, D. Zhu, L. Song, H. Zhang, X.G. Leng, TAT-LHRH conjugated low molecular weight chitosan as a gene carrier specific for hepatocellular carcinoma cells, Int. J. Nanomed. 9 (2014) 2879–2889.
[30] N. Beheshti, S. Soflaei, M. Shakibaie, M.H. Yazdi, F. Ghaffarifar, A. Dalimi, A.R. Shahverdi, Efficacy of biogenic selenium nanoparticles against *Leishmania major*: *in vitro* and *in vivo* studies, J. Trace Elem. Med. Biol. 27 (3) (2013) 203–207.
[31] A.M. Allahverdiy, E.S. Abamor, M. Bagirova, C.B. Ustundag, C. Kaya, F. Kaya, M. Rafailovich, Antileishmanial effect of silver nanoparticles and their enhanced antiparasitic activity under ultraviolet light, Int. J. Nanomed. 6 (2011) 2705–2714.
[32] A. Sazgarnia, Kh. Mayelifar, A.R. Taheri, O. Rajabi, Inhibition of Leishmania Major Growth by Ultraviolet Radiation B with Silver Nanoparticles in an Animal Model, Advanced in Nano, Biomechanics, Robotics and Energy Research (ANBRE13), Seoul, Korea, 2013, pp. 25–28.
[33] M. Delavari, A. Dalimi, F. Ghaffarifar, J. Sadraei, In Vitro Study on cytotoxic effects of ZnO nanoparticles on promastigote and amastigote forms of *Leishmania major* (MRHO/IR/75/ER), Iran. J. Parasitol. 9 (1) (2014) 6–13.
[34] N. Torabi, M. Mohebali, A.R. Shahverdi, S.M. Rezayat, G.H. Edrissian, J. Esmaeili, S. Charehdar, Nanogold for the treatment of zoonotic cutaneous leishmaniasis caused by *Leishmania major* (MRHO/IR/75/ER): an animal trial with methanol extract of Eucalyptus camaldulensis, J. Pharm. Health Sci. 1 (1) (2012) 13–16.
[35] D. Liu, J.E. Uzonna, The early interaction of *Leishmania* with macrophages and dendritic cells and its influence on the host immune response, Front. Cell Infect. Microbiol. 2 (2012) 83.